Accepted Manuscript

Antitubercular activity of 1,2,3-triazolyl fatty acid derivatives

Diego G. Ghiano, Agustina de la Iglesia, Nina Liu, Peter J. Tonge, Héctor R. Morbidoni, Guillermo R. Labadie

PII: S0223-5234(16)30822-4

DOI: 10.1016/j.ejmech.2016.09.086

Reference: EJMECH 8952

To appear in: *European Journal of Medicinal Chemistry*

Received Date: 29 June 2016

Revised Date: 24 September 2016

Accepted Date: 26 September 2016

Please cite this article as: D.G. Ghiano, A. de la Iglesia, N. Liu, P.J. Tonge, H.R. Morbidoni, G.R. Labadie, Antitubercular activity of 1,2,3-triazolyl fatty acid derivatives, *European Journal of Medicinal Chemistry* (2016), doi: 10.1016/j.ejmech.2016.09.086.

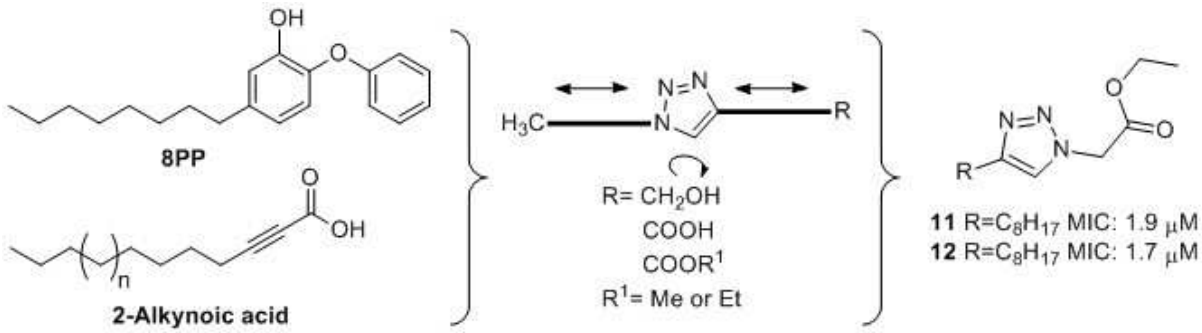

Antitubercular activity of 1,2,3-triazolyl fatty acid derivatives

Diego G. Ghiano,[a] Agustina de la Iglesia,[b] Nina Liu,[c] Peter J. Tonge,[c] Héctor R. Morbidoni,[d,e] and Guillermo R. Labadie.[a,f]*

[a] Instituto de Química Rosario, UNR, CONICET, Suipacha 531, S2002LRK, Rosario, ARGENTINA.

[b] Cátedra de Microbiología, Virología y Parasitología, Facultad de Ciencias Médicas, Universidad Nacional de Rosario, Santa Fe 3100,S2002KTR, Rosario, ARGENTINA.

[c] Institute of Chemical Biology & Drug Discovery, Department of Chemistry, Stony Brook University, Stony Brook, NY 11794, USA.

[d] Consejo de Investigaciones, Universidad Nacional de Rosario, ARGENTINA.

[e] Laboratorio de Microbiología Molecular. Facultad de Ciencias Médicas, Universidad Nacional de Rosario, Santa Fe 3100, S2002KTR, Rosario, ARGENTINA.

[f] Departamento de Química Orgánica, Facultad de Ciencias Bioquímicas y Farmacéuticas, Universidad Nacional de Rosario, Suipacha 531, S2002LRK, Rosario, ARGENTINA.

*Corresponding author

E-mail: labadie@iquir-conicet.gov.ar

Phone number: +54-341-4370477 # 108

FAX number: +54-341-4370477 # 112

Highlights

A collection of different 1,2,3-triazolyl fatty acids derivatives were prepared.

The most active compounds displayed a *M. tuberculosis* MIC below 2 µM.

Compound **11** had the same MIC towards a set of clinically isolated resistant strains.

Abstract

A collection of 1,2,3-triazoles unsaturated fatty acid mimics were efficiently synthesized by click chemistry. The 1,4-disubstituted analogs prepared covered different alkyl chain lengths and triazole positions. The compounds were subsequently tested against *Mycobacterium tuberculosis*, being most of them active with some of the analogs displaying activity at micromolar concentration. The most potent member of the series has the triazole moiety on the C-2 position with a carbon chain of eight or ten carbon atoms. The 1,5-isomers of the most active analog were significantly less active than the original isomer. The activity of the selected hit was assayed on several clinical MTB multi-drug resistant strains providing the same MIC.

1. Introduction

Tuberculosis (TB) has become the most prevalent disease in the world today, ever more than any other time in human history. This disease caused by *Mycobacterium tuberculosis* (MTB) has plagued mankind for centuries being the greatest single infectious cause of mortality worldwide, killing roughly two million people annually.[1] The treatment of multidrug resistant tuberculosis (MDR-TB) patients thus requires the administration of second line drugs like amikacin, kanamycin, capreomycin, cycloserine, para-aminosalicylic acid, ethionamide, and fluoroquinolones. Unfortunately, these drugs are less efficient and frequently more toxic requiring longer treatment times. Another drawback is that the MDR-TB treatment can cost up to 100 times higher than the basic six-month short-course chemotherapy regimen.[2] Estimates have shown that one-third of the world's population is infected with latent *M. tuberculosis*. That scenario has been increasingly aggravated due to the resistance on the drugs routinely used to treat the disease. Last statistical data published by WHO revealed the existence of a 3.5% of MDR strains worldwide and that rate has not changed.[1] Extensively drug resistant strains known as XDR, are resistant to isoniazid and rifampin, plus any fluoroquinolone and at least one of three injectable second-line drugs.[3] The resurgence of TB among immune compromised individuals, such as those with diabetes necrosis or those infected with HIV, is alarming due to the development of pathogenic synergy.[4] The scenario has turned dramatic considering that over the last 40 years no new antitubercular drug has been developed.[5] That complicated situation has prompted WHO to declare tuberculosis as a global public health crisis.[1] This has created an urgent need to develop fast acting new antitubercular drugs with diverse and unique structural features. Recently, things have turned around with bedaquiline being approved by the U.S. Food and Drug Administration (FDA) under the name Sirturo in 2012, and by the European Medicine Agency (EMA) in 2014 for the treatment of MDR-TB patients.[6]

Mycobacteria are surrounded by a thick waxy cell wall that is thought to impact the ability of many common antibiotics to reach the mycobacterial cytoplasm. Key components of these cell walls are mycolic acids, which are very long chain (C60-C90) α- branched chain fatty acids esterified to the arabinogalactan component of the cell wall or to trehalose.[7] The mycobacterial mycolic acid biosynthesis pathway (FAS-II) represents a validated and well exploited target for drug discovery.[8] The most common FAS-II enzyme targets are the enoyl ACP reductase FabI (InhA), that catalyze the last step in fatty acid elongation, and the ketoacyl-ACP synthases that catalyzes the first step, the condensation of acetyl-CoA with malonyl-ACP. Isoniazid is the current front line tuberculosis treatment regimen. This hydrazide inhibites InhA after its activation by KatG, resulting in the formation of an adduct with NAD^+. InhA inhibitors that do not require activation by KatG are effective against most INH-resistant MTB.[9] Over the last 20 years many InhA inhibitors have been reported being an attractive target to develop new antitubercular drugs.[10]

The discovery of TMC207, a first-in-class diarylquinoline compound with a novel mechanism of action,[11] has trigger the research of heterocycles as antitubercular agents. That finding was followed by different heterocycles scaffolds as promising structures to develop chemotherapies.[12-14]

One strategy to introduces heterocycles into the molecular scaffold is the use of 1,2,3-triazoles. That approach requires the incorporation of 1,2,3-triazoles into a drug candidate, as a key part of the pharmacophore, or to link several molecular portions together.[15, 16] The emerging field of click chemistry offers a unique approach to the synthesis of 1,2,3-triazole-containing molecules. It becomes popular for medicinal chemistry because azides and alkynes are practically inert to most biological and organic conditions, water, molecular oxygen, and the majority of common reaction conditions in organic synthesis. Another key advantage that turns then in an attractive connection unit is that they are stable to metabolic degradation and capable of hydrogen bonding, which can

be favorable in the binding of biomolecular targets and can improve the solubility.[17] Over the years, many examples of biologically active 1,2,3-triazole-containing molecules have been reported, including antiparasite,[18, 19] antifungal, [20] anticancer,[21] antiviral,[22, 23] and against many bacterial species.[24, 25] The synthesis of collections of 1,2,3-trizoles to develop new chemical entities toward *M. tuberculosis* has not been an exception. Different authors have reported new compounds that display promising *in vitro* activities against MTB.[26-36] (**Figure 1**)

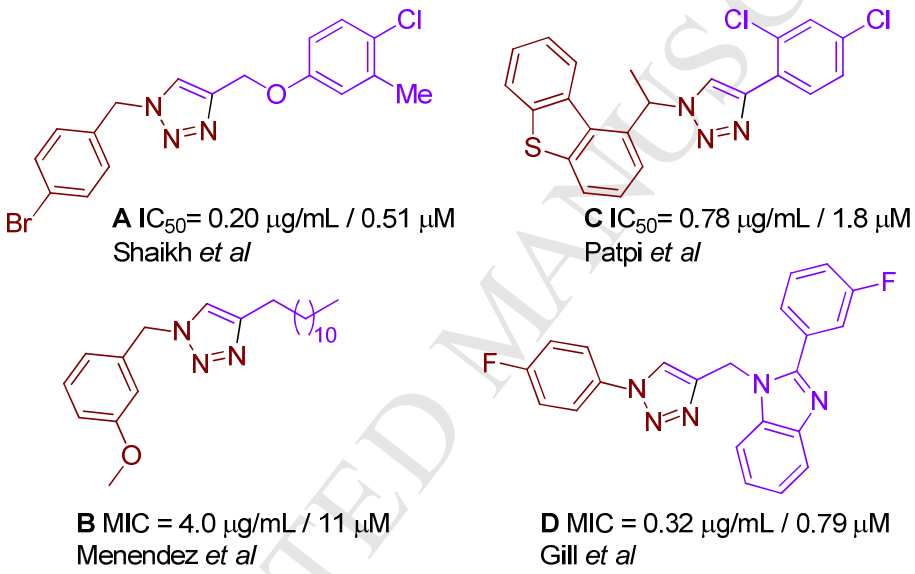

Figure 1. Antitubercular 1,2,3-triazole containing products

On a previous exploratory report[37] we have designed a collection of compounds based on the critical role displayed by fatty acid biosynthesis and metabolism and the renewed interest on triazoles as antimycobacterial drugs. Inspired on the structures of the antitubercular compounds **8PP**[38] and 2-alkynoic acid[39] we have prepared and screened a series of 1,4-disubtituted 1,2,3-triazoles. (**Figure 2**)

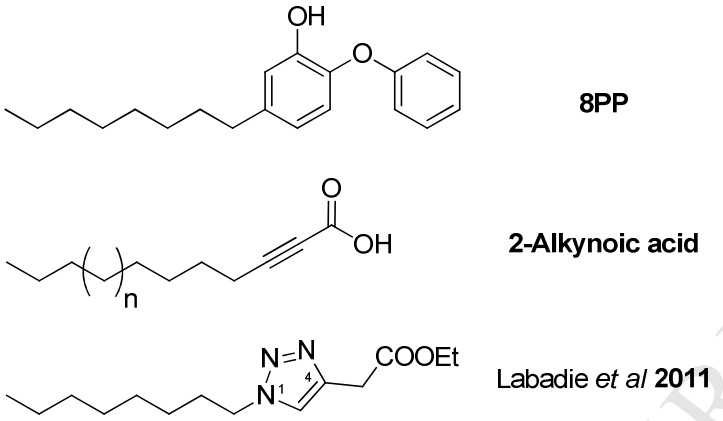

Figure 2. Strategy previously followed for library design. [37]

The antimycobacterial activity of that collection showed a clear tendency where the most active compounds have alkyl chain and ethyl acetoxy as N1 and C4 triazole substituents, respectively. Based on those results we wanted to expand that study, preparing a new library to look into the relationship between the triazole position and the activity of the previously found antimycobacterial products. On the initial study only a series of analogs with C4 alkyl substituents of 3, 5 and 8 carbon atom chain were reported. In this work, we wanted to increase the chain length up to 24 carbon atoms. (**Figure 3**)

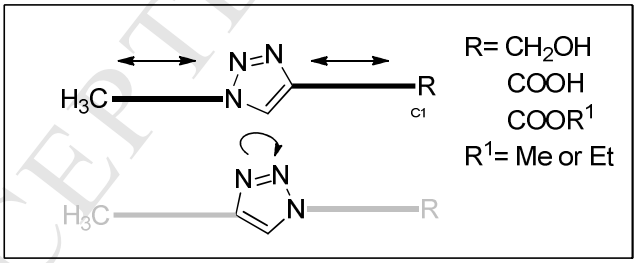

Figure 3. Structural diversity explored in this work.

Additionally, the general structure of the most active compounds resembles unsaturated fatty acids, being the triazole as isoster of the triple bond present on alkynoic acids. Based on that assumption, the position of the triazole on the carbon chain was not explored before, requiring the synthesis of analogs with different carbon length moving the triazole along the chain. Also, the

connectivity of the 1,2,3-triazole was investigated by adding analogs with the nitrogen connected to the chain close to C1. (**Figure 3**) To determine the structure-activity relationship in the present study, the activity of novel 1,4-disubstituted 1,2,3-triazole derivatives were evaluated against *M. tuberculosis* H37Rv as well as their *in vitro* cytotoxicity.

2. Results and Discussion

2.1. Chemistry

A set of new analogs were designed to evaluate the structural requirements for the activity. Based on structure of the unsaturated fatty acid substrate for InhA, three different factors were evaluated: the chain length, the triazole position and the functional group on the head. That hypothesis has been experimentally validated on other scaffolds,[40, 41] but not for unsaturated fatty acids. Molecular modeling studies were performed to corroborate that the replacement on the unsaturated fatty ester by 1,2,3-triazoles displays an equivalency to an allylic group (**Figure 4**). In the case of unsaturated *Z*-fatty ester there is some difference on the geometry compared with the 1,4-disubtituted 1,2,3- triazole, with an angle of 155.4° and a distance of 5.04 Å for the substituents of the heterocycle. Those values are close to the 179.0° measured on the *E*-double bond substituents having a shorter distance of 3.92 Å between them. For the 1,5 disubtituted-1,2,3- triazole the angle is 76.2° and the distance is 3.18 Å, being very close to the 75.4° and the 3.18 Å on the *Z* double bond. These results suggested that 1,5-disubstituted 1,2,3-triazole perfectly mimics the topology of a *Z*-double bond, meanwhile the 1,4- disubstituted regioisomer share similar topology but longer than a double bond, being equivalent to fatty acids one carbon longer.

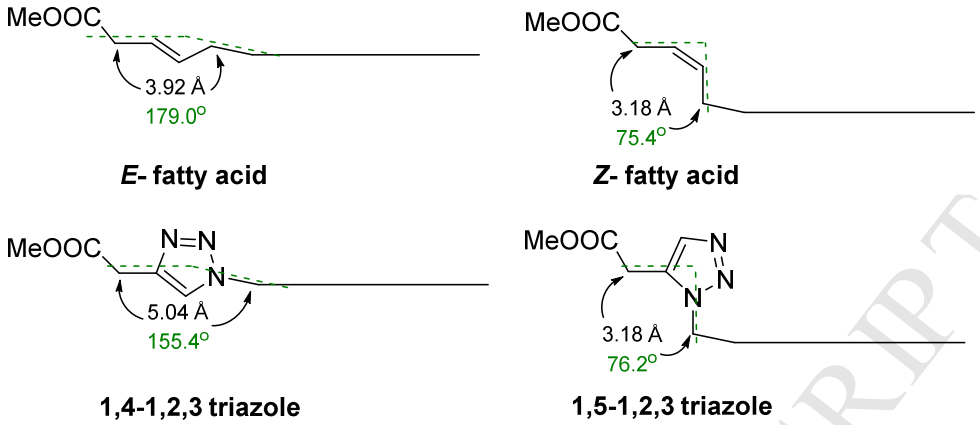

Figure 4. Comparison between unsaturated fatty esters and 1,2,3-triazole regioisomers

Compounds holding ethyl and methyl carboxylate, free carboxylic acid, and alcohols were prepared covering fatty acid chain length from C8 to C20. The position of the 1,2,3-triazole was also moved from C2 to C7. To prepare the collection, the necessary azides were synthesized by direct substitution with sodium azide in DMF starting from commercially available ω-bromo ethylesters of fatty acids from 2 to 5 carbon length. With these azides in hand, a series of 1,2,3-triazole derivatives were synthesized using commercial 1-alkynes from different carbon length. (**Scheme 1**) On the other side, starting from methyl propiolate, propiolic acid and propargyl alcohol a series of new products were prepared by Cu(I) catalyzed 1,3-dipolar cycloaddition with different aliphatic azides.

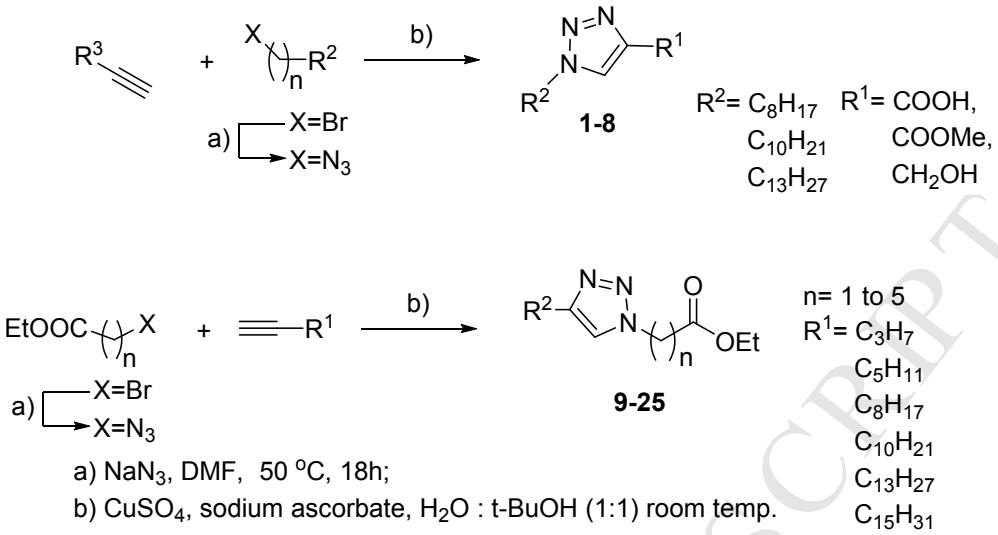

Scheme 1. Synthesis of Fatty acids 1,2,3-triazoles mimics.

All the reactions were conducted in a parallel solution synthesis fashion setup under copper(II) sulphate catalytic conditions in water:*t*-BuOH (1:1) using sodium ascorbate as reductant. The collection of triazolyl fatty esters **1**-**25** was obtained with an 80 % average yield after purification (**Table 1**). The products were characterized by 1D-, 2D- NMR experiments, IR and HRMS, displaying a 1,4-substitution pattern as was expected based our previous experience[18, 37] and by several other reports. [42, 43]

2.2. Biological evaluation

2.2.1. *In vitro* activity against *M. tuberculosis*

The prepared collection was assayed *in vitro* against *M. tuberculosis* H37rv obtaining the MIC by serial micro dilution colorimetric assay using MTT as viability indicator.[44, 45] The results are presented in the **Table 1** and are organized based on the chain length equivalence, the substituent on C1 and the 1,2,3-triazole position. The results are presented following the chain length and the position of the 1,2,3-triazole. From the left to the right the chain length increases and from the top to the bottom the position of the 1,2,3-triazole moves away from C1.

The analysis of the activity on **Table 1** showed that thirteen of the new prepared compounds have MIC below 60 μM, if the three previously reported analogs are added (**9**-**11**) the number increases to sixteen that is a 65 % of the collection. Twelve compounds displayed MICs of 25 μM or less with only four analogs above that value. The elevated number of active analogs of the library revealed the privileged character of the structure prepared.

The structure-activity relationship analysis indicates the importance of the chain length. In fact, analogs equivalent to fatty acids equivalency between twelve to fifteen carbon atoms are the most active. In that region there are ten compounds (**4**, **5**, **7**, **11**, **12**, **15**, **17**, **20**, **22**, **24**) with activities below 25 μM that is 71% of the total prepared. The majority of the most active analogs are esters, with the exception of acids **4** and **5** (MIC 14 and 20 μM), also the activity seems to be insensitive to the heterocycle position, as **7**, **15** and **24** (MIC 23, 22 and 22 μM respectively) displayed almost the same MIC having the 1,2,3-triazole on C2, C4 orC7 position. The other point of diversity incorporated was the functional group on C1, which consists of alcohols, acids and esters. From those, the alcohols seem to be the less active of the series, followed by the acids; being the esters which performed best. It is important to point out that acids were difficult to dissolve, preventing the study of longer analogs, even with the interesting profile they displayed.

An attractive series included analogs **9** to **14**, esters having the 1,2,3-triazole on C3 and different chain length that included **11,** the most active compounds of our previous work.[37] These analogs included the previously reported **9**-**11** and the longer analogs **12** to **14**. This series allowed us to conclude that the activity is heavily dependent on the chain length, with a minimum MIC for the analog **T12** (C19, MIC 1.7 μM) that is slightly more active than **11** (C17, MIC 1.9 μM). **13** (C22, MIC 296 μM) and **14 (**C24, MIC 17 μM) **,** were 174 and 10 times less active than **11**, respectively.

As a main conclusion it is clear that the combination of the triazole position on C3 (compounds with n=1, **Figure 1**) with a chain length between 17 and 19 increases the antimycobacterial activity

at least ten times. It has been reported[46] that fatty acids of 14 carbon atoms were considerably more active than their neighbors of C12 and C16. Contrary to our results, in the same article the respective esters were completely inactive, but the activity on C18 fatty acids increased along with the degree of unsaturation.

Table 1. Antimycobacterial activity of the compounds prepared.

Comp.	**n**	**R^1**	**R^2**	Yield[a]	*M. tuberculosis* MIC (μM)[b]									
1	-	CH_2OH	C_8H_{17}	72			473							
2	-	CH_2OH	$C_{10}H_{21}$	66					209					
3	-	CH_2OH	$C_{13}H_{27}$	85								44		
4	-	COOH	C_8H_{17}	86			14							
5	-	COOH	$C_{10}H_{21}$	91					20					
6	-	COOMe	C_8H_{17}	73			52							
7	-	COOMe	$C_{10}H_{21}$	83					23					
8	-	COOMe	$C_{13}H_{27}$	78								323		
9	1	-	C_3H_7	[c]	505									
10	1	-	C_5H_{11}	[c]		111								
11	1	-	C_8H_{17}	[c]				1.9						
12	1	-	$C_{10}H_{21}$	86						1.7				
13	1	-	$C_{13}H_{27}$	91									296	
14	1	-	$C_{15}H_{31}$	85										17
15	2	-	C_8H_{17}	72					22					
16	2	-	$C_{10}H_{21}$	60							20			
17	3	-	C_5H_{11}	80			12							
18	3	-	C_8H_{17}	90						21				
19	3	-	$C_{10}H_{21}$	90								309		
20	4	-	C_5H_{11}	82				23						
21	4	-	C_8H_{17}	74							40			
22	4	-	$C_{10}H_{21}$	92									37	
23	5	-	C_3H_7	78			394							
24	5	-	C_5H_{11}	72					22					
25	5	-	C_8H_{17}	77								309		
Length[d]					C12	C14	C16	C17	C18	C19	C20	C21	C22	C24

[a] %, after purification
[b] *M. tuberculosis* H37rv
[c] Previously reported[37]
[d] Equivalency to linear fatty acids

It seems possible that the activity displayed by our collection is caused by a synergetic effect between the ester and the triazole, which not only gives rigidity to the chain. A possible additional

role may involve another specific effect, different from the double bond replacement. Besides the general use of 1,2,3-triazoles as a linker or structural mimetic of aromatic rings, there are examples where there behavior exceeds that role. It has been observed on crystal structures of 1,2,3-triazole inhibitor-protein complexes that nitrogen´s triazole forms hydrogen bond with specific residues of the amino acids on the active site of the protein contributing to their stabilization.[47, 48]

The antimicrobial activity of long chain fatty acids have also been reported, being markedly influenced by the number of carbon atoms present in the alkanol chain and the presence of unsaturations.[49] In the case of *M. tuberculosis* the activity of primary linear alcohols from C6 to C11 have been recently reported.[50] The alcohols are considerably less active than the corresponding acids, being 1-decanol the most active with MIC of 800 µM. A different report explored longer-chain alcohols that displayed an antimycobacterial activity with MIC of 5 µg/mL for C12 (27 µM), C14 (23 µM) and C16 (21 µM).[51] The activity of the alcohol **1** to **3** range from 473 to 44 µM are considerably less active than the corresponding fatty alcohols, indicating that the triazoles have a negative effect on the activity.

The reported activity of alkynoic acids on *M. smegmatis*[39] has some interesting coincidence with some of our results. In that work it was demonstrated that among the analogs with the alkyne on C2, the 2-octadecynoic acid was the most active, that matches the molecular area what is the molecular area of our most potent analogs. From a series of octadecynoic acids with the triple bond between C2 to C5, 2-octadecynoic acid was the most active. In our case, the series members with the triazole moiety on C2 were considerably less active (compounds **6**-**8**), probably suggesting a different target than for 2-alkynoic acids. The activity of long fatty acids amide has also been reported.[52] The activity of those compounds was not as good as the corresponding ester, with

no members of the collection showing MIC below 12.5 μM. Those results are another indication that low polarity and lipophilicity do not provide active compounds without specific interactions.

Having completed the analysis of the influence on the chain length, the position of the triazole and the functional group requirements on C1, it was necessary to determine if the substitution pattern on the triazole may affect the activity. With that idea in mind, the 1,5-disubstituted analogs (**26** and **27**) of compounds **11** and **12** were prepared using the same precursors. Azides and alkynes were refluxed in benzene under $CP^*Ru(PPh_3)_2Cl$ catalysis following Jia´s procedure.[53] The reaction was not completely selective in our hands[54] and produced, in both cases, a mixture the 1,5- and 1,4-1,2,3-triazoles in a 4:1 ratio, respectively.(**Scheme 2**) Fortunately, both isomers were separable, characterizing the 1,5 product by comparison with previously prepared 1,4-analog and by nOe experiments. The new analogs **26** and **27** were evaluated against *M. tuberculosis* H37rv being manifestly less active than their 1,4 regioisomer. Triazole **26** has an MIC of 93 μM, meanwhile that of **27** was 84 μM, being both 1,5-isomers 49 times less active than the corresponding 1,4. Those results clearly define another important structural feature required for the pharmacophore.

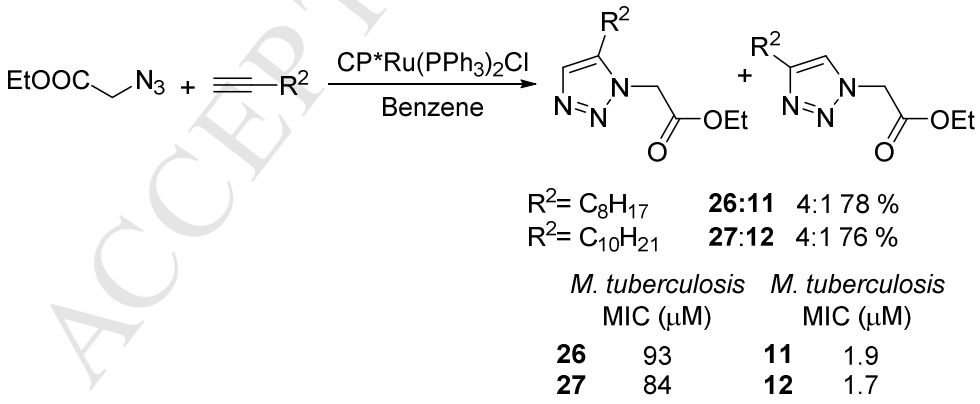

Scheme 2. Synthesis and antitubercular activity of 1,5-derivatives of the 1,2,3-triazoles most active analogs**.**

2.2.2 *In vitro* activity against *Mt* InhA.

Having in mind that the library has been inspired on the InhA inhibitor 8PP reported by Sullivan *et al,*[38] analogs **9**, **10**, **11** and **12** were assayed on the mycobacterial enzyme InhA. The assay was performed at a fixed enzyme concentration of 20 μM determining the reaction velocity in absence $(v)_0$ and presence of the inhibitor $(v)_I$ The results showed that the inhibition is very poor for the most potent mycobacterial analog **12** with 99.3 % of enzyme activity and the analog **9** with 69% of enzyme activity remaining, which is the least active of the four collection members assayed.(**Table 2**)

The reported enoyl reductases inhibitors are divided based on whether they form a covalent adduct with the NAD^+ cofactor.[55] Based on their structure the prepared analogs should not require activation by the mycobacterial KatG enzyme. A comparison between the assayed analogs and FabI/InhA experimentally validated inhibitors revealed that functional groups that should interact with critical amino acids on the active pocket are not present. Triclosan and their diphenyl ether inspired InhA analogs contain a phenolic hydroxyl on their structure. The interaction between this hydroxyl group and the Tyr158 is critical for the inhibition as can be seen on their crystal structure (2B37.pdb,[38]). The 1,2,3-triazole will probably display similar interactions and the long fatty acid tail will probably fill the hydrophobic pocket but those interactions do not provide the required stabilization energy to inhibit the enzyme. Many structurally different compounds have shown to inhibit FabI,[55] including unsaturated fatty acids. Palmitoleic, oleic, linoleic, linolenic and arachidonic acids inhibited FabI with an average IC_{50} of 40 μM being at least 50 time more active that their saturated counterpart and their esters.[56] The binding of those compounds is facilitated by their carboxylate being more suitable to inhibit the enzyme than 1,2,3-triazolyl analogs.

Therefore, it is clear that InhA is not the main molecular target of the prepared compounds as they

are, having at best, a minor contribution on the activity profile of the triazolyl fatty esters activity. In spite of that, although unlikely, mycobacterial metabolism of the compounds may be required for activity display, thus activity on inhA over-expressing *M. tuberculosis* strains would finally clarify this point. Thus, the action mechanism of the compounds is a matter of future studies. We believe that based on the scaffold of the compounds it may be connected to the mycobacterial lipid metabolism.

Table 2. Enzyme inhibition values of the selected analogs.

Comp. [a]	MIC μM	% Remaining activity[b]
9	505	69.0
10	111	73.2
11	1.9	90.1
12	1.7	99.3

[a] [Inh] = 20 μM

[b]InhA remaining activity = v_i / v_0

2.2.3 *In vitro* cytotoxicity assay on Vero cells.

The prepared compounds were assayed against Vero cells (kidney Green monkey) to determine the selectivity against the mycobacteria. All the compounds were non-cytotoxic at the maximum concentration tested of 4.75 μg/mL. Taking in consideration those values, the selected hits of the series compounds **11** (cytotoxicity IC_{50}>17.8 μM) and **12** (cytotoxicity IC_{50}> 16.1 μM) have a therapeutic index that higher than 10 which is very promising[57] being good candidate to move to further *in vivo* studies.

2.2.4 ADME-Tox calculations

One third of new chemical entities failed before reaching clinical trial phase due to poor pharmacokinetics. The required good oral availability can be achieved by balancing their partitioning and solubility properties. To rationalize the profile of our analogs computational

studies of all the synthesized compounds were performed to predict their adsorption, distribution, metabolism and excretion (ADME) properties, Lipinski's rule of five, toxicity liabilities and drug likeness. The calculation were performed using the web-based software Molinspiration,[58]and Osiris.[59] The Molinspiration platform uses a sum of fragment-based contributions and correction factors being able to calculate parameters of most of the organic and even organometallic molecules. According to Lipinski's rule of five a potential drug candidate molecule should be orally active if their molecular weight is $\leq$ 500 Da, log*P* $\leq$ 5, the number of hydrogen bond acceptors $\leq$ 10 and the number of hydrogen bond donors $\leq$ 5. The analysis of the collection revealed that all the compound have a MW<500 (187 to 365 Da), there are 8 that violated the rule with logP > 5, and all fulfill the restrictions on the number of hydrogen donors (4 or 5) and acceptors (0 or 1). Since an antimycobacterial drug has to cross the waxy mycobacterial cell wall, it is usual to find a correlation between the compound activity and its partition coefficient, with the more lipophilic being more active. A chart correlating the log (MIC μM) vs log*P* did not have a connection for all the compounds, but it was clear that two set of compounds followed a linear correlation as was expected.(**Figure 5, red** and **blue,** respectively) An interesting outcome of this chart is the location of compounds **11** and **12**. Those are the most active compounds and did not follow the same behavior than the rest of the collection. The fact that those compounds are considerable more active due to their lipophilicity could be the result of a specific interaction with an unknown molecular target than enhance their activity beyond their partition coefficient.

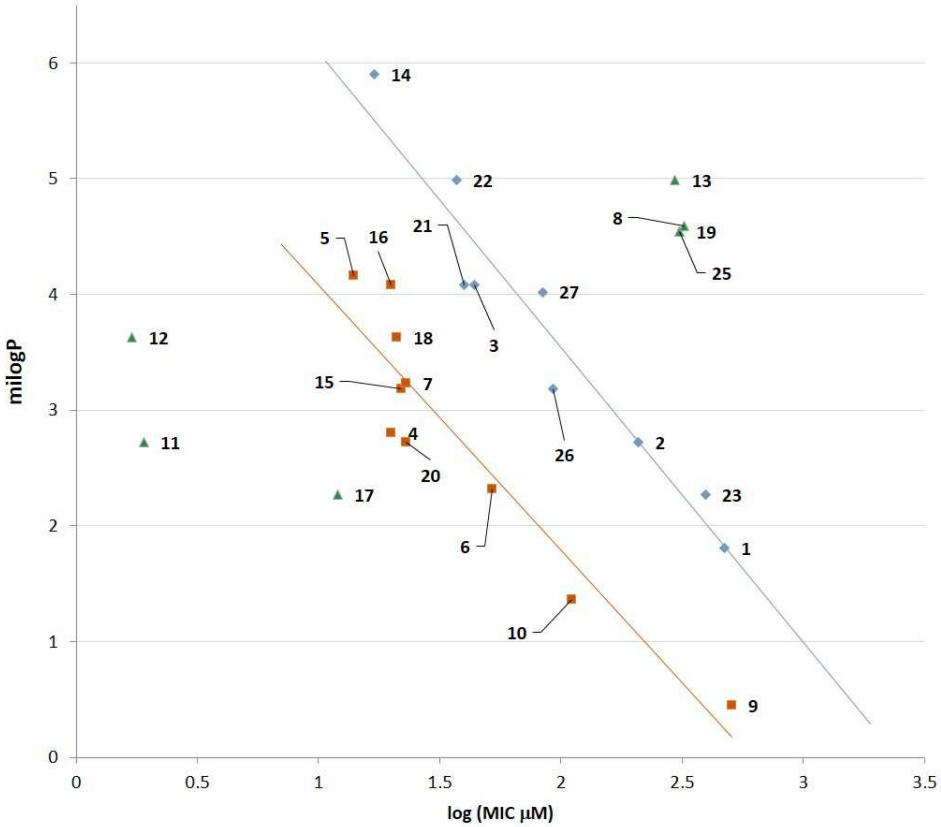

Figure 5.Correlation between log*P* and antitubercular activity.

The analysis by the Osiris platform provided the toxicity risk, drug likeness and a drug score. The results revealed that all the compounds did not have any toxicity risk, undesired effects; tumorigenic features or effect on the reproductive system. The solubility is a critical property which aids in the circulation of a drug after the administration and into the bloodstream. More than 80% of marketed drugs have logS > -4. The Osiris estimation, measured in mol/liter, provides a promising range of -4.32 to -1.62 for the studied 1,2,3-triazoles. In terms of drug likeness the prepared collection displayed a poor profile on (-9.70 to -39.79) compared to commercial drugs like fluconazole or rifampicin (1.99 and 10.5 respectively). That poor behavior is balanced with the rest of the parameters used to calculate the drug score (solubility, logP, MW and toxicity risk) delivering moderate to good values compared with a standard drug (0.25 to 0.49).

A detailed analysis of compounds **11** and **12** shown that **11** has a better drug score (0.45 vs 0.41), is more soluble (-1.73 vs -2.97), has lower MW (267.37 vs 295.43), logP (3.97 vs 4.98) and equal drug likeness. Considering that both compounds have almost the same antimycobacterial potency, it promotes **11** as the selected candidate for future studies.

2.2.7 Activity of **11** on *M. tuberculosis* drug resistant strains

As was mentioned before, the appearance of resistant *M. tuberculosis* strains is a major problem for TB treatment. For that reason, we evaluated the activity of the most promising analog, triazole **11**, on different antibiotic resistant strains. The compound was assayed on a panel of 19 clinical isolates that were resistant to rifampicin, streptomycin, isoniazid, pyrazinamide or their combinations.(**Table 3**) As can be seen, the compound maintained its potency (MIC 1.9 μM)on pansusceptible strains (**164**, **304**, **598;** except strain **51** that was more sensitive),the rifampicin resistant strains (**110**, **277**, **300**, **925** and **958**)and the isoniazid resistant strains (**277b** and **620**). The compound was equally potent toward the MDR strains (**396**, **681**, **780**, **914**, **675**)**,** showing uneven behavior on the two triple-resistant strains (**122** is more sensitive and **501** less active). However, in MIC for both strains are in a narrow concentration range and could be explain by strain differences unrelated to the susceptibility to compound **11**.

In summary, the compound maintained the activity on most of the 15 clinically isolated strains indicating that the resistance mechanisms present in the clinical isolates do not affect **11**.

Table 3. Activity of **11** on different resistant and multiresistant *M. tuberculosis* strains.

Strain	Resistance	MIC μM	Strain	Resistance	MIC μM
H37Rv	-	1.9	**277b**	Inh	1.9
51	-	0.45	**620**	Inh	1.9
164	-	1.9	**396**	Inh-Sm	1.9
304	-	1.9	**681**	Inh-Sm	1.9
598	-	1.9	**780**	Inh-Sm	1.9
110	Rif	1.9	**914**	Inh-Sm	1.9
277	Rif	1.9	**675**	Rif -Sm	1.9
300	Rif	1.9	**122**	Rif-Inh-Pza	0.9
925	Rif	1.9	**501**	Rif-Inh-Pza	3.7
958	Rif	1.9			

a) Rif= rifampicin, Sm=streptomycin, Inh= isoniazid, Pza=pyrazinamide

3. Conclusions

In the present study a set of twenty five 1,5-subtituted-1,2,3-triazolyl fatty esters were prepared with good yields. The collection was assayed against *M. tuberculosis* H37rv and thirteen of the newly prepared compounds have MIC of below 60 μM. The activity profile of the series allowed to reach a well-defined structural-activity relationship that in turn allowed setting the structural requirements that define a new antimycobacterial scaffold. The pharmacophore requirements are described on the **Figure 6**. To maximize their activity the compounds have to contain an ester on C1, the triazole has to have a 1,4-alkyl-substitution that has to be between C17 to C19 long. The studies conducted to validate the target of **11** revealed that are not linked to InhA inhibition. Also, **11** activity was not affected by the resistant mechanisms to rifampicin, streptomycin, isoniazid and pyrazinamide present in clinical isolates. In general, the prepared compounds showed suitable drug score and good ADME-tox properties and are expected to present good bioavailability profile. In summary, **11** has emerged as a valuable candidate considering its simple preparation and its high potency. The possibility that their activity could target pathway(s) different than the ones targeted by standard therapeutic antimycobacterial drugs encourages further mechanistic studies and additional exploration of structural modifications with enhanced activity.

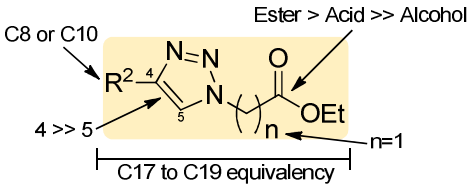

Figure 6. Structural requirements for activity.

4. Material and methods

4.1. General

Chemical reagents were purchased from commercial suppliers and were used without further purification unless otherwise noted. All the solvents (hexane, ethyl acetate, CH_2Cl_2, Et_2O) were distilled prior to use. Yields were calculated for material judged homogenous by thin layer chromatography and nuclear magnetic resonance (NMR). Reaction progress was monitored by thin layer chromatography (TLC) performed on silica gel 60 F_{254} pre-coated aluminum sheets. Spots were visualized under 254 nm UV lamp and/or by dipping the TLC plate into a solution of p-anisaldehyde or phosphomolibdic acid followed by heating with a heat gun. Flash column chromatography was performed using silica gel 60 (230 – 400 mesh). ^{1}H and ^{13}C NMR spectra were recorded in a Bruker Avance II 300 MHz (75.13 MHz) using $CDCl_3$ as solvent unless otherwise noted. Chemical shifts for proton nuclear magnetic resonance (^{1}H NMR) spectra are reported in parts per million relative to the signal of tetramethylsilane at 0 ppm (internal standard) and coupling constants (*J*) are reported in hertz (Hz). Chemical shifts for carbon nuclear magnetic resonance (^{13}C NMR) spectra are reported in parts per million relative to the center line of the $CDCl_3$triplet at 76.9 ppm. Assignments of proton resonances were confirmed by correlated spectroscopy. ESI-HRMS were recorded at the University of Mississippi, Department of Medicinal Chemistry on a Waters LC-QTof micro.

4.2. Synthesis

4.2.1. General procedure for Azides and Alkynes reaction under click chemistry conditions:

Alkyne (1 eq) and the azide (1 eq) were suspended in mL/eq of t-BuOH:H_2O (1:1) and then aqueous 1M $CuSO_4$ solution and finally aqueous 1M sodium ascorbate solution were added and the mixture stirred overnight at room temperature. Brine was added and the solution was extracted with dichloromethane. Combined organic extracts were dried with sodium sulphate and evaporated. The resulting residue was purified by column chromatography over silica gel using an increasing AcOEt/hexane gradient to afford desired pure products.

4.2.1.1. (1-octyl-1*H*-1,2,3-triazol-4-yl)methanol (**1**)

White solid. M.p. 49.0-49.8 °C. ^{1}H NMR (300 MHz, $CDCl_3$): δ7.50 (s, 1H), 4.79 (s, 2H), 4.33 (t, *J* = 7.3 Hz, 2H), 1.91-1.85 (m, 2H), 1.65 (m, 2H), 1.31-1.25 (m, 10H), 0.87 (t, *J* = 6.3 Hz, 3H).^{13}C NMR (75 MHz, $CDCl_3$): δ147.5 (C), 121.4 (CH), 56.7 (CH_2), 50.4 (CH_2), 31.7 (CH_2), 30.3 (CH_2), 29.0 (CH_2), 28.9 (CH_2), 26.5 (CH_2), 22.6 (CH_2), 14.0 (CH_3), IR (KBr) υ: 3400, 2953, 2922, 2852, 1651, 1465, 1220, 1145 cm^{-1}. ESI-HRMS Calcd for ($M+H^+$) $C_{11}H_{21}N_3O$ 212.1763, found 212.1768.

4.2.1.2. (1-decyl-1*H*-1,2,3-triazol-4-yl)methanol (**2**)

White solid. Mp: 61.3-61.0 °C. ^{1}H NMR (300 MHz, $CDCl_3$): δ 7.51 (s, 1H), 4.79 (s, 2H), 4.34 (t, *J* = 7.3 Hz, 2H), 1.89 (q, *J* = 5.8 Hz, 2H), 1.67-1.50 (m, 2H), 1.31-1.25 (m, 18H), 0.87 (t, *J* = 6.3 Hz, 3H).^{13}C NMR (75 MHz, $CDCl_3$): δ130.9 (C), 121.4 (CH), 56.6 (CH_2), 50.4 (CH_2), 31.7 (CH_2), 30.3 (CH_2), 29.0 (CH_2), 27.7 (CH_2), 19.2 (CH_2), 22.6 (CH_2), 14.0 (CH_3). IR (KBr) υ: 3385, 2954, 2920, 2846, 1730, 1462, 1274, 1122, 1072, 746 cm^{-1}. ESI-HRMS Calcd for ($M+H^+$) $C_{13}H_{26}N_3O$ 240.2076, found 240.2083.

4.2.1.3. (1-tridecyl-1*H*-1,2,3-triazol-4-yl)methanol (**3**)

White solid. M.p. 78.8-79.6 °C. ^{1}H NMR (300 MHz, $CDCl_3$): δ 7.51 (s, 1H), 4.79 (s, 2H), 4.34 (t, *J* = 7.2 Hz, 2H), 1.92-1.87 (m, 2H), 1.68 (m, 2H), 1.31-1.25 (m, 20H), 0.87 (t, *J* = 6.3 Hz, 3H).^{13}C NMR (75 MHz, $CDCl_3$): δ 121.4 (C), 56.6 (CH_2), 50.4 (CH_2), 31.9 (CH_2), 30.3 (CH_2), 9.6 (CH_2), 29.5 (CH_2), 29.4

(CH_2), 29.3 (CH_2), 29.0 (CH_2), 26.5 (CH_2), 22.7 (CH_2), 14.1 (CH_3). IR (KBr) υ: 3415, 2918, 2847, 1643, 1465, 1274, 860, 750 cm^{-1}. ESI-HRMS Calcd for ($M+H^+$) $C_{16}H_{32}N_3O$ 282.2545, found 282.2539.

4.2.1.4. 1-octyl-1H-1,2,3-triazole-4-carboxylic acid (**4**)

White solid. Mp: 158.8-159.5 °C.^{1}H NMR (300 MHz, DMSO-d_6): δ 8.68 (s, 1H), 4.37 (t, *J* = 7.0 Hz, 2H), 3.35 (t, *J* = 4.5 Hz, 2H), 1,83 (q, *J* = 10.8 Hz, 2H), 1.23 (m,12H), 0.83 (t, *J* = 6.9 Hz, 3H).^{13}C NMR (75 MHz, DMSO): δ 161.2 (C), 139.0 (C), 128.2 (CH), 49.1 (CH_2), 30.6 (CH_2), 28.9 (CH_2), 27.9 (CH_2), 27.7 (CH_2), 25.1 (CH_2), 21.5 (CH_2), 13.4 (CH_3). IR (KBr) 3117, 2957,2920, 2848, 2355, 1681, 1467, 1234, 1047, 602 cm^{-1}. ESI-HRMS Calcd for ($M+H^+$) $C_{11}H_{20}N_3O_2$ 226.1556, found 226.1546.

4.2.1.5. 1-decyl-1H-1,2,3-triazole-4-carboxylic acid (**5**)

White solid. M.p. 150.4-151.1 °C. ^{1}H NMR (300 MHz, DMSO): δ 8.67 (s, 1H), 4.37 (t, *J* = 6.4 Hz, 2H), 3.35 (t, *J* = 4.5 Hz, 2H), 1,80 (t, *J* = 12.8 Hz, 2H), 1.21 (m, 14H), 0.85 (t, *J* = 6.3 Hz, 3H).^{13}C NMR (75 MHz, DMSO): δ161.7 (C), 139.5 (C), 128.7 (CH), 60.7 (CH_2), 49.6 (CH_2), 31.2 (CH_2), 29.4 (CH_2), 28.8 (CH_2), 28.8 (CH_2), 28.6 (CH_2), 28.2 (CH_2), 25.6 (CH_2), 22.0 (CH_2), 13.9 (CH_3). IR (KBr) 3117, 2359, 1541, 1465, 1339, 1234, 1045, 779 cm^{-1}. ESI-HRMS Calcd for ($M+Na^+$) $C_{13}H_{23}N_3O_2Na$ 276.1688, found 276.1680.

4.2.1.6. Methyl 1-octyl-1*H*-1,2,3-triazole-4-carboxylate (**6**)

White solid. M.p. 75.7-76.5 °C. ^{1}H NMR (300 MHz, $CDCl_3$): δ 8.07 (s, 1H), 4.40 (t, *J* = 7.2 Hz, 2H), 3.95 (s, 3H), 1.97-1.90 (m, 2H), 1.62 (s, 2H), 1.31-1.26 (m, 10H), 0.87 (t, *J* = 6.3 Hz, 3H).^{13}C NMR (75 MHz, $CDCl_3$): δ161.3 (C), 139.9 (C), 127.2 (CH), 52.2 (CH_2), 50.7 (CH_2), 31.6 (CH_2), 30.1 (CH_2), 29.0 (CH_2), 28.9 (CH_2), 26.3 (CH_2), 22.6 (CH_2), 14.0 (CH_3). IR (KBr) υ: 3120, 2953, 2914, 2846, 1730, 1539, 1469, 1384, 1348, 1234, 1047, 881, 777 cm^{-1}. ESI-HRMS Calcd for ($M+H^+$) $C_{12}H_{21}N_3O_2$ 240.1712, found 240.1724.

4.2.1.7. Methyl 1-decyl-1*H*-1,2,3-triazole-4-carboxylate (**7**)

White solid. M.p. 95.4-96.0 °C. ^{1}H NMR (300 MHz, $CDCl_3$): δ 8.07 (s, 1H), 4.40 (t, *J* = 7.2 Hz, 2H), 3.95 (s, 3H), 1.92 (q, *J* = 6.4 Hz, 2H), 1.31-1.24 (m, 18H), 0.87 (t, *J* = 6.3 Hz, 3H).^{13}C NMR (75 MHz, $CDCl_3$): δ 161.3 (C), 139.9 (C), 127.2 (CH), 52.2 (CH_3), 50.7 (CH_2), 31.8 (CH_2), 30.1 (CH_2), 29.4 (CH_2), 29.3 (CH_2), 29.2 (CH_2), 28.9 (CH_2), 26.3 (CH_2), 22.6 (CH_2), 14.1 (CH_3). IR (KBr) υ: 3130, 2999, 2958, 2358, 1753, 1726, 1543, 1377, 1022, 871, 779 cm^{-1}. ESI-HRMS Calcd for ($M+H^+$) $C_{14}H_{26}N_3O_2$ 268.2025, found 268.2015.

4.2.1.8. Methyl 1-tridecyl-1H-1,2,3-triazole-4-carboxylate (**8**)

White solid. Mp: 96.2-96.9 °C. ^{1}H NMR (300 MHz, $CDCl_3$): δ 8.07 (s, 1H), 4.39 (t, *J* = 7.2 Hz, 2H), 3.94 (s, 3H), 1.92 (q, *J* = 6.9 Hz, 2H), 1.31-1.24 (m, 20H), 0.87 (t, *J* = 6.3 Hz, 3H).^{13}C NMR (75 MHz, $CDCl_3$): δ 161.3 (C), 139.9 (C), 127.2 (CH), 52.2 (CH_3), 50.7 (CH_2), 31.9 (CH_2), 31.3 (CH_2), 29.6 (CH_2), 29.6 (CH_2), 29.5 (CH_2), 29.3 (CH_2), 28.9 (CH_2), 26.4 (CH_2), 22.7 (CH_2), 14.1 (CH_3). IR (KBr) υ: 3120, 2915, 2846, 2355, 1732, 1543, 1468, 1242, 1051, 777, 719 cm^{-1}. ESI-HRMS Calcd for ($M+H^+$) $C_{17}H_{32}N_3O_2$ 310.2495, found 310.2491.

4.2.1.9. Ethyl 2-(4-decyl-1H-1,2,3-triazol-1-yl)acetate (**12**)

White solid. Mp: 61.1-62.0 °C. ^{1}H NMR (300 MHz, $CDCl_3$): δ 7.40 (s, 1H), 5.11 (s, 2H), 4.26 (q, *J* = 7.1 Hz, 2H), 2.73 (t, *J* = 7.7 Hz, 3H), 1.70-1.63 (m, 3H), 1.29 (t, *J* = 7.1 Hz, 3H), 1.26 (m, 16H), 0.88 (t, *J* = 6.7 Hz, 3H).^{13}C NMR (75 MHz, $CDCl_3$): δ 166.7 (C), 149.2 (C), 122.1 (CH), 62.5 (CH_2), 51.0 (CH_2), 32.1 (CH_2), 29.9 (CH_2), 29.8 (CH_2), 29.6 (CH_2), 29.4 (CH_2), 25.9 (CH_2), 22.9 (CH_2), 14.3 (CH_3), 14.3 (CH_3). IR (KBr) υ: 3122, 3064, 2954, 2918, 2848, 1745, 1467, 1377, 1220, 1055, 1033, 721 cm^{-1}. ESI-HRMS Calcd for ($M+H^+$) $C_{16}H_{30}N_3O_2$ 296.2338, found 296.2341.

4.2.1.10 Ethyl 2-(4-tridecyl-1H-1,2,3-triazol-1-yl)acetate (**13**)

White solid. M.p. 70.2-71.1 °C.^{1}H NMR (300 MHz, $CDCl_3$): δ 7.40 (s, 1H), 5.11 (s, 2H), 4.26 (q, *J* = 7.1 Hz, 2H), 2.73 (t, *J* = 7.8 Hz, 3H), 1.70-1.62 (m, 2H), 1.29-1.25 (m, 26H), 0.87 (t, *J* = 6.6 Hz, 3H).^{13}C

NMR (75 MHz, $CDCl_3$):δ 166.7 (C), 149.1 (C), 122.1 (CH), 62.5 (CH_2), 50.9 (CH_2), 32.1 (CH_2), 29.8 (CH_2), 29.7 (CH_2), 29.5 (CH_2), 29.4 (CH_2), 25.8 (CH_2), 22.9 (CH_2), 14.3 (CH_3), 14.2 (CH_3). IR (KBr) υ: 3064, 2953, 2916, 2848, 1745, 1469, 1456, 1375, 1220, 1055, 1035, 719 cm^{-1}. ESI-HRMS Calcd for ($M+H^+$) $C_{19}H_{36}N_3O_2$ 338.2808, found 338.2808.

4.2.1.11. Ethyl 2-(4-pentadecyl-1H-1,2,3-triazol-1-yl)acetate (**14**)

White solid. Mp: 76.2-77.1 °C.^{1}H NMR (300 MHz, $CDCl_3$): δ 7.39 (s, 1H), 5.11 (s, 2H), 4,25 (q, *J* = 7.1 Hz, 2H), 2.73 (t, *J* = 7.8 Hz, 3H), 1.69-1.65 (m, 3H), 1.29 (t, *J* = 14.3 Hz, 3H), 1.25 (m, 23H), 0.87 (t, *J* = 6.3 Hz, 3H).^{13}C NMR (75 MHz, $CDCl_3$): δ166.7 (C), 149.1 (C), 122.1 (CH), 62.5 (CH_2), 51.0 (CH_2), 32.1 (CH_2), 29.9 (CH_2), 29.7 (CH_2), 29.5 (CH_2), 29.4 (CH_2), 25.8 (CH_2), 22.9 (CH_2), 14.3 (CH_3), 14.23 (CH_3). IR (KBr) υ: 3064, 2954, 2916, 2848, 1747, 1469, 1222, 1197, 1056 cm^{-1}. ESI-HRMS Calcd for ($M+H^+$) $C_{21}H_{40}N_3O_2$ 336.3121, found 366.3136.

4.2.1.12. Ethyl 3-(4-octyl-1H-1,2,3-triazol-1-yl)propanoate (**15**)

Colourless oil. ^{1}H NMR (300 MHz, $CDCl_3$): δ 7.34 (s, 1H), 4.60 (t, *J* = 6.4 Hz, 2H), 4.15 (q, *J* = 7.1 Hz, 2H), 2.94 (t, *J* = 6.6 Hz, 2H), 2.68 (t, *J* = 8.1 Hz, 2H), 1.67-1.59 (m, 7H), 1.28 (m, 14H), 1.24 (t, *J* = 7.1 Hz, 3H), 0.87 (t, *J* = 6.6 Hz, 3H).^{13}C NMR (75 MHz, $CDCl_3$): δ 170.6 (C), 148.3 (C), 121.4 (CH), 61.1 (CH_2), 45.3 (CH_2), 34.8 (CH_2), 31.8 (CH_2), 29.4 (CH_2), 29.3 (CH_2), 29.2 (CH_2), 29.1 (CH_2), 25.6 (CH_2), 22.6 (CH_2), 14.0 (CH_3). IR (film) υ: 2956, 2852, 1732, 1552, 1446, 1195, 1018, 945, 858, 723 cm^{-1}. ESI-HRMS Calcd for ($M+H^+$) $C_{15}H_{28}N_3O_2$ 282.2182, found 282.2192.

4.2.1.13. Ethyl 3-(4-decyl-1H-1,2,3-triazol-1-yl)propanoate (**16**)

White solid. Mp:43.1-44.0 °C. ^{1}H NMR (300 MHz, $CDCl_3$): δ 7.34 (s, 1H), 4.60 (t, *J* = 6.4 Hz, 2H), 4,15 (q, *J* = 7.0 Hz, 2H), 2.93 (t, *J* = 6.5 Hz, 2H), 2.68 (t, *J* = 7.5 Hz, 2H), 1.67-1.59 (m, 7H), 1.26 (t, *J* = 7.1 Hz, 3H), 1.25 (m, 14H), 0.87 (t, *J* = 6.9 Hz, 3H).^{13}C NMR (75 MHz, $CDCl_3$): δ170.6 (C), 148.3 (C), 121.4 (CH), 61.1 (CH_2), 45.3 (CH_2), 34.8 (CH_2), 31.8 (CH_2), 29.4 (CH_2), 29.3 (CH_2), 29.2 (CH_2), 29.1 (CH_2),

25.6 (CH_2), 22.6 (CH_2), 14.0 (CH_3). IR (KBr) υ: 2926, 2854, 1753, 1556, 1456, 1375, 1211, 1026, 987, 819 cm^{-1}. ESI-HRMS Calcd for ($M+H^+$) $C_{17}H_{32}N_3O_2$ 310.2495, found 310.2502.

4.2.1.14. Ethyl 4-(4-pentyl-1H-1,2,3-triazol-1-yl)butanoate (**17**)

Colourless oil. ^{1}H NMR (300 MHz, $CDCl_3$): δ 7.26 (s, 1H), 4.38 (t, *J* = 6.8 Hz, 2H), 4,13 (q, *J* = 7.1 Hz, 2H), 2.69 (t, *J* = 7.5 Hz, 2H), 2.32 (t, *J* = 6.6 Hz, 2H), 2.25-2.15 (m, 2H), 1.68-1.63 (m, 3H), 1.35-1.30 (m, 4H), 1.28 (t, *J* = 7.2 Hz, 3H), 0.89 (t, *J* = 6.6 Hz, 3H). ^{13}C NMR (75 MHz, $CDCl_3$): δ172.3 (C), 148.4 (C), 120.7 (CH), 60.5 (CH_2), 48.9 (CH_2), 31.3 (CH_2), 30.7 (CH_2), 29.0 (CH_2), 25.5 (CH_2), 25.4 (CH_2), 22.3 (CH_2), 14.1 (CH_3), 13.9 (CH_3). ESI-HRMS Calcd for ($M+H^+$) $C_{13}H_{24}N_3O_2$ 254.1869, found 254.1861.

4.2.1.15. Ethyl 4-(4-octyl-1H-1,2,3-triazol-1-yl)butanoate (**18**)

White solid. M.p. 42.7-43-3 °C.^{1}H NMR (300 MHz, $CDCl_3$): δ 7.26 (s, 1H), 4.38 (t, *J* = 6.8 Hz, 2H), 4,13 (q, *J* = 7.1 Hz, 2H), 2.69 (t, *J* = 8.0 Hz, 2H), 2.32 (t, *J* = 6.6 Hz, 2H), 2.25-2.15 (m, 2H), 1.68-1.60 (m, 3H), 1.31-1.26 (m, 10H), 1.25 (t, *J* = 7.2 Hz, 3H), 0.87 (t, *J* = 6.6 Hz, 3H). ^{13}C NMR (75 MHz, $CDCl_3$): δ 172.3 (C), 148.5 (C), 120.7 (CH), 60.6 (CH_2), 49.0 (CH_2), 31.8 (CH_2), 30.7 (CH_2), 29.4 (CH_2), 29.3 (CH_2), 29.2 (CH_2), 25.6 (CH_2), 25.5 (CH_2), 25.6 (CH_2), 22.6 (CH_2), 14.1 (CH_3), 14.0 (CH_3). IR (KBr) υ: 3109, 3057, 2918, 2850, 1732, 1467, 1215, 1184, 1053, 871, 806, 721 cm^{-1}. ESI-HRMS Calcd for ($M+H^+$) $C_{16}H_{30}N_3O_2$ 296.2338, found 296.2331.

4.2.1.16. Ethyl 4-(4-decyl-1H-1,2,3-triazol-1-yl)butanoate (**19**)

White solid. M.p. 49.1-49.8 °C. ^{1}H NMR (300 MHz, $CDCl_3$): δ7.26 (s, 1H), 4.38 (t, *J* = 6.8 Hz, 2H), 4.13 (q, *J* = 7.1 Hz, 2H), 2.69 (t, *J* = 7.5 Hz, 2H), 2.32 (t, *J* = 6.6 Hz, 2H), 2.25-1.17 (m, 2H), 1.67-1.62 (m, 2H), 1.31-1.24 (m, 14H), 1.25 (t, *J* = 14.3 Hz, 3H), 0.87 (t, *J* = 6.3 Hz, 3H). ^{13}C NMR (75 MHz, $CDCl_3$): δ172.3 (C), 148.4 (C), 120.6 (CH), 60.5 (CH_2), 48.9 (CH_2), 31.8 (CH_2), 30.7 (CH_2), 29.5 (CH_2), 29.5 (CH_2), 29.4 (CH_2), 29.3 (CH_2), 29.2 (CH_2), 29.2 (CH_2), 25.6 (CH_2), 25.4 (CH_2), 22.6 (CH_2), 14.1 (CH_3), 14.0 (CH_3). IR (KBr) υ: 2927, 2856, 1759, 1554, 1462, 1375, 1209, 1026, 819 cm^{-1}.

4.2.1.17. Ethyl 5-(4-pentyl-1H-1,2,3-triazol-1-yl)pentanoate (**20**)

Colourless oil. ^{1}H NMR (300 MHz, $CDCl_3$): δ7.25 (s, 1H), 4.33 (t, *J* = 6.8 Hz, 2H), 4.69 (q, *J* = 7.1 Hz, 2H), 2.70 (t, *J* = 7.5 Hz, 2H), 2.33 (t, *J* = 6.6 Hz, 2H), 1.99-1.89 (m, 2H), 1.67-1.61 (m, 4H), 1.33 (m, 4H), 1.24 (t, *J* = 7.1 Hz, 3H), 0.89 (t, *J* = 6.9 Hz, 3H). ^{13}C NMR (75 MHz, $CDCl_3$): δ172.9 (C), 148.4 (C), 120.5 (CH), 60.4 (CH_2), 49.6 (CH_2), 33.4 (CH_2), 31.4 (CH_2), 29.6 (CH_2), 29.1 (CH_2), 25.6 (CH_2), 22.3 (CH_2), 21.8 (CH_2), 14.1 (CH_3), 13.9 (CH_3). IR (film) υ: 2954, 2931, 2358, 1732, 1458, 1375, 1182, 1047, 1029 cm^{-1}. ESI-HRMS Calcd for (M+H$^+$) $C_{14}H_{26}N_3O_2$ 268.2025, found 268.2038.

4.2.1.18. Ethyl 5-(4-octyl-1H-1,2,3-triazol-1-yl)pentanoate (**21**)

Colourless oil. ^{1}H NMR (300 MHz, $CDCl_3$): δ 7.24 (s, 1H), 4.31 (t, *J* = 7.1 Hz, 2H), 4,11 (q, *J* = 7.1 Hz, 2H), 2.69 (t, *J* = 7.5 Hz, 2H), 2.33 (t, J = 7.2 Hz, 2H), 1.98-1.88 (m, 2H), 1.67-1.61 (m, 4H), 1.25 (m, 10H), 1.24 (t, *J* = 7.0 Hz, 3H), 0.87 (t, *J* = 6.6 Hz, 3H). ^{13}C NMR (75 MHz, $CDCl_3$): δ 173.0 (C), 148.5 (C), 120.5 (CH), 60.4 (CH_2), 49.7 (CH_2), 33.4 (CH_2), 31.9 (CH_2), 29.7 (CH_2), 29.5 (CH_2), 29.3 (CH_2), 29.3 (CH_2), 29.2 (CH_2), 25.7 (CH_2), 22.7 (CH_2), 21.8 (CH_2), 14.2 (CH_3), 14.1 (CH_3). IR: 3134, 2957, 2936, 2870, 2359, 1730, 1551, 1462, 1373, 1213, 1182, 1034 cm^{-1}. ESI-HRMS Calcd for (M+H$^+$) $C_{17}H_{32}N_3O_2$ 310.2495, found 310.2501.

4.2.1.19. Ethyl 5-(4-decyl-1H-1,2,3-triazol-1-yl)pentanoate (**22**).

White solid. M.p. 46.9-47.9 °C.^{1}H NMR (300 MHz, $CDCl_3$): δ7.25 (s, 1H), 4.32 (t, *J* = 7.1 Hz, 2H), 4.12 (q, *J* = 7.1 Hz, 2H), 2.69 (t, *J* = 7.5 Hz, 2H), 2.33 (t, *J* = 7.3 Hz, 2H), 1.99-1.89 (m, 2H), 1.69-1.62 (m, 4H), 1.26 (m, 14H), 1.25 (t, *J* = 7.1 Hz, 3H), 0.88 (t, *J* = 6.6 Hz, 3H).^{13}C NMR (75 MHz, $CDCl_3$): δ172.9 (C), 148.4 (C), 120.5 (CH), 60.3 (CH_2), 49.6 (CH_2), 33.4 (CH_2), 31.8 (CH_2), 29.6 (CH_2), 29.5 (CH_2), 29.5 (CH_2), 29.4 (CH_2), 29.3 (CH_2), 29.2 (CH_2), 25.66 (CH_2), 22.6 (CH_2), 21.8 (CH_2), 14.2 (CH_3), 14.04 (CH_3). IR (KBr) υ: 3055, 2918, 2848, 1730, 1552, 1469, 1267, 1029, 736 cm^{-1}. ESI-HRMS Calcd for (M+H$^+$) $C_{19}H_{36}N_3O_2$338.2808, found 338.2800.

4.2.1.20. Ethyl 6-(4-propyl-1H-1,2,3-triazol-1-yl)hexanoate (**23**)

Colourless oil. ^{1}H NMR (300 MHz, $CDCl_3$): δ 7.24 (s, 1H), 4.30 (t, *J* = 7.1 Hz, 2H), 4.10 (q, *J* = 7.1 Hz, 2H), 2.68 (t, *J* = 7.5 Hz, 2H), 2.28 (t, *J* = 7.4 Hz, 2H), 1.95-1.85 (m, 2H), 1.73-1.62 (m, 4H), 1.73-1.62 (m, 4H), 1.37 (m, 2H), 1.23 (t, *J* = 7.2 Hz, 3H), 0.95 (t, *J* = 7.3 Hz, 3H).^{13}C NMR (75 MHz, $CDCl_3$): δ173.3 (C), 148.1 (C), 120.6 (CH), 60.2 (CH_2), 49.8 (CH_2), 33.9 (CH_2), 30.0 (CH_2), 27.6 (CH_2), 25.9 (CH_2), 24.2 (CH_2), 22.6 (CH_2), 14.2 (CH_3), 13.7 (CH_3). IR (film) υ: 2956, 2935, 2870, 2358, 1730, 1550, 1462, 1373, 1213, 1182, 1033 cm^{-1}. ESI-HRMS Calcd for ($M+H^+$) $C_{13}H_{24}N_3O_2$ 254.1869, found 254.1874

4.2.1.21. Ethyl 6-(4-pentyl-1H-1,2,3-triazol-1-yl)hexanoate (**24**)

Colourless oil. ^{1}H NMR (300 MHz, $CDCl_3$): δ7.24 (s, 1H), 4.30 (t, *J* = 7.1 Hz, 2H), 4.11 (q, *J* = 7.1 Hz, 2H), 2.70 (t, *J* = 7.5 Hz, 2H), 2.29 (t, *J* = 7.4 Hz, 2H), 1.95-1.85 (m, 2H), 1.73-1.62 (m, 4H), 1.71-1.61 (m, 4H), 1.40-1.29 (m, 6H), 1.24 (t, *J* = 7.1 Hz, 3H), 0.89 (t, *J* = 6.9 Hz, 3H).^{13}C NMR (75 MHz, $CDCl_3$): δ173.3 (C), 148.4 (C), 120.5 (CH), 60.3 (CH_2), 49.8 (CH_2), 33.9 (CH_2), 31.4 (CH_2), 30.0 (CH_2), 29.1 (CH_2), 25.9 (CH_2), 25.6 (CH_2), 24.2 (CH_2), 22.4 (CH_2), 14.2 (CH_3), 14.0 (CH_3). IR (film) υ: 3134, 2931, 2858, 1730, 1550, 1462, 1373, 1180, 1047 cm^{-1}. ESI-HRMS Calcd for ($M+H^+$) $C_{15}H_{28}N_3O_2$ 282.2182, found 282.2194.

4.2.1.22. Ethyl 6-(4-octyl-1H-1,2,3-triazol-1-yl)hexanoate (**25**)

Colourless oil. M.p. 34.2-35.0 °C.^{1}H NMR (300 MHz, $CDCl_3$): δ 7.24 (s, 1H), 4.30 (t, *J* = 7.2 Hz, 2H), 4,11 (q, *J* = 7.1 Hz, 2H), 2.69 (t, *J* = 7.8 Hz, 2H), 2.29 (t, *J* = 7.4 Hz, 2H), 1.95-1.85 (m, 2H), 1.71-1.63 (m, 4H), 1.34-1.26 (m, 12H), 1.25(t, *J* = 7.1 Hz, 3H), 0.87 (t, *J* = 6.3 Hz, 3H).^{13}C NMR (75 MHz, $CDCl_3$): δ173.4 (C), 148.5 (C), 120.5 (CH), 60.3 (CH_2), 49.9 (CH_2), 34.0 (CH_2), 31.9 (CH_2), 30.1 (CH_2), 29.5 (CH_2), 29.4 (CH_2), 29.3 (CH_2), 29.3 (CH_2), 26.0 (CH_2), 25.7 (CH_2), 24.3 (CH_2), 22.7 (CH_2), 14.3 (CH_3), 14.1 (CH_3). IR (film) υ: 2926, 2854, 2358, 1735, 1463, 1375, 1180, 1047 cm^{-1}. ESI-HRMS Calcd for ($M+H^+$) $C_{18}H_{34}N_3O_2$ 324.2651, found 324.2660

4.2.2. General procedure for $Cp^*RuCl(PPh_3)_2$ catalyzed reactions:

A solution of ethyl 2-azidoacetate (1.3 eq) and alkyne (1 eq) in benzene was added to $Cp^*RuCl(PPh_3)_2$ (0.01 eq) dissolved in 2.5 mL of dioxane. The vial was purged with nitrogen, sealed, and heated in an oil bath at 60 °C for 12 h, at which point TLC indicated complete consumption of the azide starting materials. The mixture was adsorbed onto silica and chromatographed with hexanes/ethyl acetate (1:1) to remove nonpolar impurities, followed by ethyl acetate to elute the desired pure products.

4.2.2.1. Ethyl 2-(5-octyl-1H-1,2,3-triazol-1-yl)acetate (**26**)

Colourless oil. ^{1}H NMR (300 MHz, $CDCl_3$): δ 7.48 (s, 1H), 5.06 (s, 2H), 4.25 (q, *J* = 7.1 Hz, 2H), 2.56 (t, *J* = 7.5 Hz, 3H), 1.28 (t, *J* = 7.1 Hz, 3H), 1.27 (m, 11H), 0.88 (t, *J* = 6.6 Hz, 3H).^{13}C NMR (75 MHz, $CDCl_3$): δ 166.3 (C), 138.3 (C), 132.2 (CH), 62.3 (CH_2), 48.8 (CH_2), 31.8 (CH_2), 29.2 (CH_2), 29.2 (CH_2), 29.1 (CH_2), 27.7 (CH_2), 23.1 (CH_2), 22.6 (CH_2), 14.1 (CH_3), 14.2 (CH_3). IR (film) υ: 2927, 2856, 1755, 1554, 1462, 1375, 1209, 1097, 1026, 987 cm^{-1}. ESI-HRMS Calcd for ($M+H^+$) $C_{14}H_{26}N_3O_2$ 268.2025, found 268.2019.

4.2.2.2.Ethyl 2-(5-decyl-1H-1,2,3-triazol-1-yl)acetate (**27**)

Colourless oil. ^{1}H NMR (300 MHz, $CDCl_3$): δ 7.47 (s, 1H), 5.05 (s, 2H), 4.23 (q, *J* = 7.1 Hz, 2H), 2.55 (t, *J* = 7.5 Hz, 3H), 1.70-1.60 (m, 3H), 1.29-1,25 (m, 17H), 0.86 (t, *J* = 6.6 Hz, 3H).^{13}C NMR (75 MHz, $CDCl_3$): δ 166.3 (C), 138.3 (C), 132.2 (CH), 62.3 (CH_2), 48.8 (CH_2), 31.9 (CH_2), 29.5 (CH_2), 29.4 (CH_2), 29.3 (CH_2), 29.2 (CH_2), 29.1 (CH_2), 27.7 (CH_2), 23.1 (CH_2), 22.7 (CH_2), 14.1 (CH_3), 14.1 (CH_3). IR (film) υ: 2926, 2854, 1755, 1556, 1462, 1375, 1300, 1244, 1211, 1095, 1026, 987 cm^{-1}. ESI-HRMS Calcd for ($M+H^+$): $C_{16}H_{29}N_3O_2$ 296.2338, found 296.2333.

4.3. Biology

4.3.1. Bacterial strains:

M. tuberculosis strain H37Rv was kindly provided by Dr. L. Barrera (Instituto Nacional de Microbiología "C.G. Malbrán", Argentina).The clinically isolates strains were from laboratory stocks.

All the mycobacterial strains were grown in Middlebrook 7H9 broth (Difco Laboratories, Detroit, MI, USA) supplemented with 1/10 v/v of ADS (a solution containing 50 g/L BSA fraction V, 20 g/L dextrose and 8.1 g/L NaCl) , glycerol (1% w/v) herein designated 7H9-ADS-G for short. Tween 80 was added to prevent clumping (0.05 % w/v for cultures of *M. tuberculosis*. When needed, solid media (Middlebrook 7H11 supplemented with ADS (1/10 v/v) and glycerol (1% v/v) was used. All strains were grown at 37 °C under gentle agitation.

4.3.2. *In vitro* compound activity against *M. tuberculosis* (Mtb)

Stock solutions for all the tested compounds were made in DMSO at 10 mg/mL. Working solutions were made by dilution in the above described 7H9 - ADS-G medium at a final concentration of 400 µg/mL.

Antimycobacterial activity was determined by a two-fold dilution of the compounds in Middlebrook 7H9-ADS-G medium. For this purpose 96-well plates (Falcon, Cat number 3072, Becton Dickinson, Lincoln Park, NJ) were used. The 96 well-plates received 100 µL of Middlebrook 7H9 broth and a serial two-fold dilution of the compounds was made directly on the plate. The initial and final drug concentrations tested were 100 µg/mL and 0.8 µg/mL, respectively. Four compounds were tested in duplicate in each microtiter plate, Rifampicin (from 2 µg/mL to 0.16 µg/mL; stock solution prepared as a 10 mg/mL solution in methanol) was used as control drug. For the sake of simplicity of the 96 wells plate design. The compounds were tested in the range of 20 µg/mL to 0.16 µg/mL and 100 µg/mL- 0.81 µg/mL, respectively. Two rows were used for growth control (medium and inoculum alone) and sterility control (medium alone). The inoculum was prepared as a 1/25 dilution of a fresh mid-log M. *tuberculosis* H37Rv suspension (O.D equivalent to

Mc Farland 1.0 scale value) made in Middlebrook 7H9-ADS-G. A 100 µL aliquot (containing approximately 10^6 Colony Forming Units) was used to inoculate the wells except for the row used for sterility testing. Plates were sealed with Parafilm and incubated at 37°C for five days. After this time, 22 µL of a freshly prepared solution of the tetrazolium dye 3-[4,5-dimethylthiazol-2-yl]-2,5-diphenyltetrazolium bromide (MTT, Sigma, 2.5 mg/mL in 1:1 water: 20% (w/v) Tween 80) was added to the first growth control well plate in the growth control row and reincubated at 37 °C for 24h. A change from yellow to purple colour indicated that the plate was ready to be fully developed in which case 22 µL of the MTT solution was added to the rest of the wells. If the colour change was not observed the second well in the growth control row was developed as describe above and incubated for a further 24 h. The operation was repeated if necessary until a colour change was clearly seen in the growth control well, at which time the remaining drug containing wells were developed. In our experience, colour change in the growth control row was seen in the first well.

Minimum Inhibitory Concentration (MIC) was defined as the lowest drug concentration preventing mycobacterial growth and colour change.

4.3.3 Cytotoxicity assay

The *in vitro* cytotoxicity was determined against mammalian kidney fibroblasts (VERO). The assay was performed in 96-well tissue culture-treated plates as described earlier.[60] Briefly, cells were seeded to the wells of the plate (25,000 cells/well) and incubated for 24 h. Samples were added and plates were again incubated for 48 h. The number of viable cells was determined by neutral red assay. IC_{50} values were determined from logarithmic graphs of growth inhibition versus concentration. Doxorubicin was used as a positive control (IC_{50} = 14 µM, Vero cells), while DMSO was used as vehicle control.

4.3.4 InhA inhibition assay

Inhibition activity was tested using trans-2-dodecenoyl-Coenzyme A (DD-CoA) and wild-type InhA as described previously.[61] Reactions were initiated by the addition of 100 nM InhA to to solutions containing 25 µM DD-CoA, 20 µM inhibitor, and 250 µM NADH in 30 mM PIPES and 150 mM NaCl, pH 6.8 buffer. Control reactions were carried out with the same conditions as described above but without inhibitor. The inhibitory activity of each derivative was expressed as the percentage inhibition of InhA activity (initial velocity of the reaction) with respect to the control reaction without inhibitor.

Acknowledgments

This work was supported in part by grants from National Research Council of Argentina, CONICET (PIP 2009-11/0796 and 2012-14/0448); Agencia Nacional de Promoción Científica y Tecnológica, ANPCyT- Argentina (PICT 2011/0589 to GRL and PICT2005/38198 to HRM), Universidad Nacional de Rosario and Fundación Josefina Prats. This investigation received financial support from the UNICEF /UNDP /WORLD BANK /WHO Special Programme for Research and Training in Tropical Diseases (TDR) to GRL. GRL is a member of the scientific staff of CONICET-Argentina. HRM is a career member of CIUNR-Argentina. D.G.G. thanks CONICET for the award of a Fellowship.

References

[1] Global Tuberculosis Report 2014, World Health Organization, Geneva, Switzerland, 2014.

[2] R. Diel, J. Vandeputte, G. de Vries, J. Stillo, M. Wanlin, A. Nienhaus, Costs of tuberculosis disease in the European Union: a systematic analysis and cost calculation, Eur. Respir. J., 43 (2014) 554-565.

[3] N.R. Gandhi, P. Nunn, K. Dheda, H.S. Schaaf, M. Zignol, D. van Soolingen, P. Jensen, J. Bayona, Multidrug-resistant and extensively drug-resistant tuberculosis: a threat to global control of tuberculosis, The Lancet, 375 (2010) 1830-1843.

[4] J.C. Sacchettini, E.J. Rubin, J.S. Freundlich, Drugs versus bugs: in pursuit of the persistent predator *Mycobacterium tuberculosis*, Nat. Rev. Microbiol., 6 (2008) 41-52.

[5] Y. Dashti, T. Grkovic, R.J. Quinn, Predicting natural product value, an exploration of anti-TB drug space, Nat. Prod. Rep,, 31 (2014) 990-998.

[6] G. Poce, M. Cocozza, S. Consalvi, M. Biava, SAR analysis of new anti-TB drugs currently in pre-clinical and clinical development, Eur. J. Med. Chem., 86 (2014) 335-351.

[7] A. Koul, E. Arnoult, N. Lounis, J. Guillemont, K. Andries, The challenge of new drug discovery for tuberculosis, Nature, 469 (2011) 483-490.

[8] D.J. Payne, M.N. Gwynn, D.J. Holmes, D.L. Pompliano, Drugs for bad bugs: confronting the challenges of antibacterial discovery, Nat. Rev. Drug Discov., 6 (2007) 29-40.

[9] P. Pan, P.J. Tonge, Targeting InhA, the FASII enoyl-ACP reductase: SAR studies on novel inhibitor scaffolds, Curr. Top. Med. Chem., 12 (2012) 672-693.

[10] O. Holas, P. Ondrejcek, M. Dolezal, *Mycobacterium tuberculosis* enoyl-acyl carrier protein reductase inhibitors as potential antituberculotics: development in the past decade, J. Enzyme Inhib. Med. Chem., 30 (2015) 629-648.

[11] A. Matteelli, A.C.C. Carvalho, K.E. Dooley, A. Kritski, TMC207: the first compound of a new class of potent anti-tuberculosis drugs, Future Microbiology, 5 (2010) 849-858.

[12] R.S. Keri, B.S. Sasidhar, B.M. Nagaraja, M.A. Santos, Recent progress in the drug development of coumarin derivatives as potent antituberculosis agents, Eur. J. Med. Chem., 100 (2015) 257-269.

[13] R.S. Keri, K. Chand, T. Ramakrishnappa, B.M. Nagaraja, Recent progress on pyrazole scaffold-based antimycobacterial agents, Arch Pharm (Weinheim), 348 (2015) 299-314.

[14] P.M. Chauhan, N. Sunduru, M. Sharma, Recent advances in the design and synthesis of heterocycles as anti-tubercular agents, Future Med Chem, 2 (2010) 1469-1500.

[15] J. Hou, X. Liu, J. Shen, G. Zhao, P.G. Wang, The impact of click chemistry in medicinal chemistry, Expert Opin. Drug Discov., 7 (2012) 489-501.

[16] S.G. Agalave, S.R. Maujan, V.S. Pore, Click Chemistry: 1,2,3-Triazoles as pharmacophores, Chem. Asian J., 6 (2011) 2696-2718.

[17] P. Thirumurugan, D. Matosiuk, K. Jozwiak, Click Chemistry for Drug Development and Diverse Chemical–Biology Applications, Chem. Rev., 113 (2013) 4905-4979.

[18] E.O. Porta, P.B. Carvalho, M.A. Avery, B.L. Tekwani, G.R. Labadie, Click chemistry decoration of amino sterols as promising strategy to developed new leishmanicidal drugs, Steroids, 79 (2014) 28-36.

[19] E.M. Guantai, K. Ncokazi, T.J. Egan, J. Gut, P.J. Rosenthal, P.J. Smith, K. Chibale, Design, synthesis and *in vitro* antimalarial evaluation of triazole-linked chalcone and dienone hybrid compounds, Biorg. Med. Chem., 18 (2010) 8243-8256.

[20] Z.-C. Dai, Y.-F. Chen, M. Zhang, S.-K. Li, T.-T. Yang, L. Shen, J.-X. Wang, S.-S. Qian, H.-L. Zhu, Y.-H. Ye, Synthesis and antifungal activity of 1,2,3-triazole phenylhydrazone derivatives, Org. Biomol. Chem., 13 (2015) 477-486.

[21] N. Ma, Y. Wang, B.X. Zhao, W.C. Ye, S. Jiang, The application of click chemistry in the synthesis of agents with anticancer activity, Drug Design, Development and Therapy, 9 (2015) 1585-1599.

[22] M. Whiting, J.C. Tripp, Y.-C. Lin, W. Lindstrom, A.J. Olson, J.H. Elder, K.B. Sharpless, V.V. Fokin, rapid discovery and structure−activity profiling of novel inhibitors of human immunodeficiency virus type 1 protease enabled by the Copper(I)-catalyzed synthesis of 1,2,3-triazoles and their further functionalization, J. Med. Chem., 49 (2006) 7697-7710.

[23] M.J. Giffin, H. Heaslet, A. Brik, Y.-C. Lin, G. Cauvi, C.-H. Wong, D.E. McRee, J.H. Elder, C.D. Stout, B.E. Torbett, A copper(i)-catalyzed 1,2,3-triazole azide−alkyne click compound is a potent inhibitor of a multidrug-resistant hiv-1 protease variant, J. Med. Chem., 51 (2008) 6263-6270.

[24] B. Garudachari, A.M. Isloor, M.N. Satyanarayana, H.-K. Fun, G. Hegde, Click chemistry approach: Regioselective one-pot synthesis of some new 8-trifluoromethylquinoline based 1,2,3-triazoles as potent antimicrobial agents, European Journal of Medicinal Chemistry, 74 (2014) 324-332.

[25] I. Dreier, L.H. Hansen, P. Nielsen, B. Vester, A click chemistry approach to pleuromutilin derivatives. Part 3: Extended footprinting analysis and excellent MRSA inhibition for a derivative with an adenine phenyl side chain, Bioorg. Med. Chem. Lett., 24 (2014) 1043-1046.

[26] C. Menendez, S. Gau, C. Lherbet, F. Rodriguez, C. Inard, M.R. Pasca, M. Baltas, Synthesis and biological activities of triazole derivatives as inhibitors of InhA and antituberculosis agents, Eur. J. Med. Chem., 46 (2011) 5524-5531.

[27] C. Menendez, A. Chollet, F. Rodriguez, C. Inard, M.R. Pasca, C. Lherbet, M. Baltas, Chemical synthesis and biological evaluation of triazole derivatives as inhibitors of InhA and antituberculosis agents, Eur. J. Med. Chem., 52 (2012) 275-283.

[28] C. Menendez, F. Rodriguez, A.L. Ribeiro, F. Zara, C. Frongia, V. Lobjois, N. Saffon, M.R. Pasca, C. Lherbet, M. Baltas, Synthesis and evaluation of alpha-ketotriazoles and alpha,beta-diketotriazoles as inhibitors of *Mycobacterium tuberculosis*, Eur. J. Med. Chem., 69 (2013) 167-173.

[29] K. Dabak, O. Sezer, A. Akar, O. Anac, Synthesis and investigation of tuberculosis inhibition activities of some 1,2,3-triazole derivatives, Eur. J. Med. Chem., 38 (2003) 215-218.

[30] S.R. Patpi, L. Pulipati, P. Yogeeswari, D. Sriram, N. Jain, B. Sridhar, R. Murthy, T. Anjana Devi, S.V. Kalivendi, S. Kantevari, Design, synthesis, and structure-activity correlations of novel dibenzo[b,d]furan, dibenzo[b,d]thiophene, and N-methylcarbazole clubbed 1,2,3-triazoles as potent inhibitors of *Mycobacterium tuberculosis*, J. Med. Chem., 55 (2012) 3911-3922.

[31] S. Kim, S.N. Cho, T. Oh, P. Kim, Design and synthesis of 1H-1,2,3-triazoles derived from econazole as antitubercular agents, Bioorg. Med. Chem. Lett., 22 (2012) 6844-6847.

[32] P. Shanmugavelan, S. Nagarajan, M. Sathishkumar, A. Ponnuswamy, P. Yogeeswari, D. Sriram, Efficient synthesis and *in vitro* antitubercular activity of 1,2,3-triazoles as inhibitors of Mycobacterium tuberculosis, Bioorg. Med. Chem. Lett., 21 (2011) 7273-7276.

[33] N. Boechat, V.F. Ferreira, S.B. Ferreira, G.F.M. de Lourdes, C.d.S.F. de, M.M. Bastos, S.C.M. Dos, M.C. Lourenco, A.C. Pinto, A.U. Krettli, A.C. Aguiar, B.M. Teixeira, N.V. da Silva, P.R. Martins, F.A. Bezerra, A.L. Camilo, G.P. da Silva, C.C. Costa, Novel 1,2,3-triazole derivatives for use against *Mycobacterium tuberculosis* H37Rv (ATCC 27294) strain, J. Med. Chem., 54 (2011) 5988-5999.

[34] C. Gill, G. Jadhav, M. Shaikh, R. Kale, A. Ghawalkar, D. Nagargoje, M. Shiradkar, Clubbed [1,2,3] triazoles by fluorine benzimidazole: A novel approach to H37Rv inhibitors as a potential treatment for tuberculosis, Bioorg. Med. Chem. Lett., 18 (2008) 6244-6247.

[35] M.H. Shaikh, D.D. Subhedar, L. Nawale, D. Sarkar, F.a. Kalam Khan, J.N. Sangshetti, B.B. Shingate, 1,2,3-Triazole derivatives as antitubercular agents: synthesis, biological evaluation and molecular docking study, Med. Chem. Commun., 6 (2015) 1104-1116.

[36] J.M. Altimari, S.C. Hockey, H.I. Boshoff, A. Sajid, L.C. Henderson, Novel 1,4-Substituted-1,2,3-Triazoles as Antitubercular Agents, ChemMedChem, 10 (2015) 787-791.

[37] G.R. Labadie, A. de la Iglesia, H.R. Morbidoni, Targeting tuberculosis through a small focused library of 1,2,3-triazoles, Mol. Divers., 15 (2011) 1017-1024.

[38] T.J. Sullivan, J.J. Truglio, M.E. Boyne, P. Novichenok, X. Zhang, C.F. Stratton, H.J. Li, T. Kaur, A. Amin, F. Johnson, R.A. Slayden, C. Kisker, P.J. Tonge, High affinity InhA inhibitors with activity against drug-resistant strains of *Mycobacterium tuberculosis*, ACS Chem. Biol., 1 (2006) 43-53.

[39] H.R. Morbidoni, C. Vilcheze, L. Kremer, R. Bittman, J.C. Sacchettini, W.R. Jacobs, Jr., Dual inhibition of mycobacterial fatty acid biosynthesis and degradation by 2-alkynoic acids, Chem. Biol., 13 (2006) 297-307.

[40] A. Tam, U. Arnold, M.B. Soellner, R.T. Raines, Protein prosthesis: 1, 5-disubstituted [1, 2, 3] triazoles as cis-peptide bond surrogates, J. Am. Chem. Soc., 129 (2007) 12670-12671.

[41] K. Odlo, J. Hentzen, J.F. dit Chabert, S. Ducki, O.A.B.S.M. Gani, I. Sylte, M. Skrede, V.A. Fløtenes, T.V. Hansen, 1,5-Disubstituted 1,2,3-triazoles as cis-restricted analogues of combretastatin A-4: Synthesis, molecular modeling and evaluation as cytotoxic agents and inhibitors of tubulin, Biorg. Med. Chem., 16 (2008) 4829-4838.

[42] R. Tiwari, P.A. Miller, L.R. Chiarelli, G. Mori, M. Šarkan, I. Centárová, S. Cho, K. Mikušová, S.G. Franzblau, A.G. Oliver, M.J. Miller, Design, syntheses, and anti-TB activity of 1,3-benzothiazinone azide and click chemistry products inspired by BTZ043, ACS Medicinal Chemistry Letters, 7 (2016) 266-270.

[43] A. Anand, R.J. Naik, H.M. Revankar, M.V. Kulkarni, S.R. Dixit, S.D. Joshi, A click chemistry approach for the synthesis of mono and bis aryloxy linked coumarinyl triazoles as anti-tubercular agents, European Journal of Medicinal Chemistry, 105 (2015) 194-207.

[44] S. Foongladda, D. Roengsanthia, W. Arjrattanakool, C. Chuchottaworn, A. Chaiprasert, S.G. Franzblau, Rapid and simple MTT method for rifampicin and isoniazid susceptibility testing of *Mycobacterium tuberculosis*, Int. J. Tuberc. Lung Dis., 6 (2002) 1118-1122.

[45] L. Caviedes, J. Delgado, R.H. Gilman, Tetrazolium microplate assay as a rapid and inexpensive colorimetric method for determination of antibiotic susceptibility of *Mycobacterium tuberculosis*, J. Clin. Microbiol., 40 (2002) 1873-1874.

[46] E. Kondo, K. Kanai, The relationship between the chemical structure of fatty acids and their mycobactericidal activity, Jpn. J. Med. Sci. Biol., 30 (1977) 171-178.

[47] T.P. Soares da Costa, W. Tieu, M.Y. Yap, N.R. Pendini, S.W. Polyak, D. Sejer Pedersen, R. Morona, J.D. Turnidge, J.C. Wallace, M.C.J. Wilce, G.W. Booker, A.D. Abell, Selective inhibition of biotin protein ligase from *Staphylococcus aureus*, J. Biol. Chem., 287 (2012) 17823-17832.

[48] L. Drouin, S. McGrath, L.R. Vidler, A. Chaikuad, O. Monteiro, C. Tallant, M. Philpott, C. Rogers, O. Fedorov, M. Liu, W. Akhtar, A. Hayes, F. Raynaud, S. Müller, S. Knapp, S. Hoelder, Structure enabled design of BAZ2-ICR, a chemical probe targeting the bromodomains of BAZ2A and BAZ2B, J. Med. Chem., 58 (2015) 2553-2559.

[49] A.P. Desbois, V.J. Smith, Antibacterial free fatty acids: activities, mechanisms of action and biotechnological potential, Appl. Microbiol. Biotechnol., 85 (2010) 1629-1642.

[50] K. Mukherjee, P. Tribedi, B. Mukhopadhyay, A.K. Sil, Antibacterial activity of long-chain fatty alcohols against mycobacteria, FEMS Microbiol. Lett., 338 (2013) 177-183.

[51] D. Pires, E. Valente, M.F. Simões, N. Carmo, B. Testa, L. Constantino, E. Anes, Esters of pyrazinoic acid are active against pyrazinamide-resistant strains of *Mycobacterium tuberculosis* and other naturally resistant mycobacteria in vitro and ex vivo within macrophages, Antimicrob. Agents Chemother., 59 (2015) 7693-7699.

[52] C.d.R. Montes D'Oca, T. Coelho, T.G. Marinho, C.R. Hack, R.d.C. Duarte, P.A. da Silva, M.G. Montes D'Oca, Synthesis and antituberculosis activity of new fatty acid amides, Bioorg. Med. Chem. Lett., 20 (2010) 5255-5257.

[53] L. Zhang, X. Chen, P. Xue, H.H. Sun, I.D. Williams, K.B. Sharpless, V.V. Fokin, G. Jia, Ruthenium-catalyzed cycloaddition of alkynes and organic azides, J. Am. Chem. Soc., 127 (2005) 15998-15999.

[54] D. Imperio, T. Pirali, U. Galli, F. Pagliai, L. Cafici, P.L. Canonico, G. Sorba, A.A. Genazzani, G.C. Tron, Replacement of the lactone moiety on podophyllotoxin and steganacin analogues with a 1,5-disubstituted 1,2,3-triazole via ruthenium-catalyzed click chemistry, Biorg. Med. Chem., 15 (2007) 6748-6757.

[55] H. Lu, P.J. Tonge, Inhibitors of FabI, an enzyme drug target in the bacterial fatty acid biosynthesis pathway, Acc. Chem. Res., 41 (2008) 11-20.

[56] C.J. Zheng, J.-S. Yoo, T.-G. Lee, H.-Y. Cho, Y.-H. Kim, W.-G. Kim, Fatty acid synthesis is a target for antibacterial activity of unsaturated fatty acids, FEBS Lett., 579 (2005) 5157-5162.

[57] P.Y. Muller, M.N. Milton, The determination and interpretation of the therapeutic index in drug development, Nat. Rev. Drug Discov., 11 (2012) 751-761.

[58] http://www.molinspiration.com. v2014.11, 20-08-2015., in.

[59] http://www.organic-chemistry.org/prog/peo/ 26/03/2014: version 2, 20-08-2015., in.

[60] H. Babich, E. Borenfreund, Cytotoxicity of T-2 toxin and its metabolites determined with the neutral red cell viability assay, Appl. Environ. Microbiol., 57 (1991) 2101-2103.

[61] L. Bonnac, G.Y. Gao, L. Chen, K. Felczak, E.M. Bennett, H. Xu, T. Kim, N. Liu, H. Oh, P.J. Tonge, K.W. Pankiewicz, Synthesis of 4-phenoxybenzamide adenine dinucleotide as NAD analogue with inhibitory activity against enoyl-ACP reductase (InhA) of *Mycobacterium tuberculosis*, Bioorg. Med. Chem. Lett., 17 (2007) 4588-4591.

List of Figures and Table captions

Figure 1. Antitubercular 1,2,3-triazole containing products

Figure 2. Strategy previously followed for library design. [37]

Figure 3. Structural diversity explored in this work.

Figure 4. Comparison between unsaturated fatty esters and 1,2,3-triazole regioisomers

Scheme 1. Synthesis of Fatty acids 1,2,3-triazoles mimics.

Table 1. Antimycobacterial activity of the compounds prepared.

[a] %, after purification
[b] *M. tuberculosis* H37rv
[c] Previously reported[37]
[d] Equivalency to linear fatty acids

Scheme 2. Synthesis and antitubercular activity of 1,5-derivatives of the 1,2,3-triazoles most active

Table 2. Enzyme inhibition values of the selected analogs.

[a] [Inh] = 20 μM

[b] InhA remaining activity = v_i / v_0

Figure 5.Correlation between log*P* and antitubercular activity.

Table 3. Activity of **11** on different resistant and multiresistant *M. tuberculosis* strains.

Figure 6. Structural requirements for activity.